

Martin Dierolf<sup>1,2</sup>, Oliver Bunk<sup>1</sup>, Søren Kynde<sup>1</sup>, Pierre Thibault<sup>1</sup>, Ian Johnson<sup>1</sup>, Andreas Menzel<sup>1</sup>, Konstantins Jefimovs<sup>1</sup>, Christian David<sup>1</sup>, Othmar Marti<sup>2</sup> and Franz Pfeiffer<sup>1,3</sup>

<sup>1</sup>Paul Scherrer Institut · CH-5232 Villigen PSI · Switzerland

<sup>2</sup>Institute for Experimental Physics, Ulm University · 89069 Ulm · Germany

<sup>3</sup>Ecole Polytechnique Fédérale de Lausanne · CH-1015 Lausanne · Switzerland

If an object is illuminated with coherent electromagnetic radiation, *e.g.* by visible laser light or highly brilliant x-rays, a diffraction pattern is formed in the Fraunhofer far field that is related via a Fourier transform to the optical transmission function of the object. The aim of *coherent diffractive imaging* (CDI), or so-called *lensless imaging*, is to directly reconstruct the original optical transmission function of the specimen from its measured diffraction pattern. In principle, CDI allows one to obtain a resolution that is ultimately limited only by the wavelength of the radiation used and not by the quality of optical lenses. In x-ray microscopy, for instance, the resolution is presently limited to several tens of nanometres because of difficulties in manufacturing efficient high-quality nano-structured x-ray optical elements. Since CDI schemes allow the resolution to be increased beyond these limits they are among the most promising techniques for x-ray imaging applications in life and materials sciences on the nanometre scale.

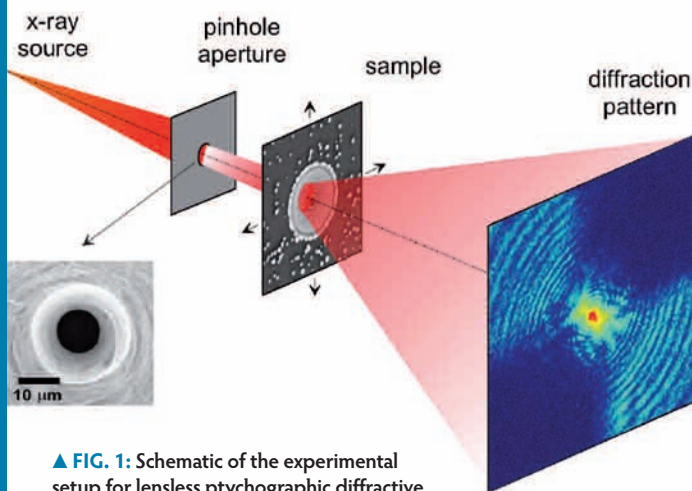
### Solution of the phase problem with iterative algorithms

A fundamental drawback of any coherent diffractive imaging method, however, is the phase problem: the measurable real-valued intensity diffraction data contain only amplitude information while the equally important phase distribution is not recorded. Fortunately, with the advent of modern computers the solution of the phase problem became feasible via certain iterative phase retrieval methods. These are algorithms alternating

between real and Fourier space while imposing certain boundary constraints on both [3,4]. They have proven useful in fields like astronomy, digital signal processing, and coherent imaging. Especially in the field of CDI, impressive results have been reported meanwhile, such as, for example, the imaging of a freeze-dried yeast cell [5], lead nanocrystals [6] and gold nano-structures [7]. Despite these promising results there are some severe principal limitations. To retrieve a unique set of phases most algorithms require the object to be very small and of a finite extent so that the corresponding highly detailed coherent diffraction pattern can be adequately sampled by the detector [3-7]. Therefore, obtaining a low-resolution overview of a comparably large area and then zooming into a region of interest - a standard procedure in microscopy - is not feasible.

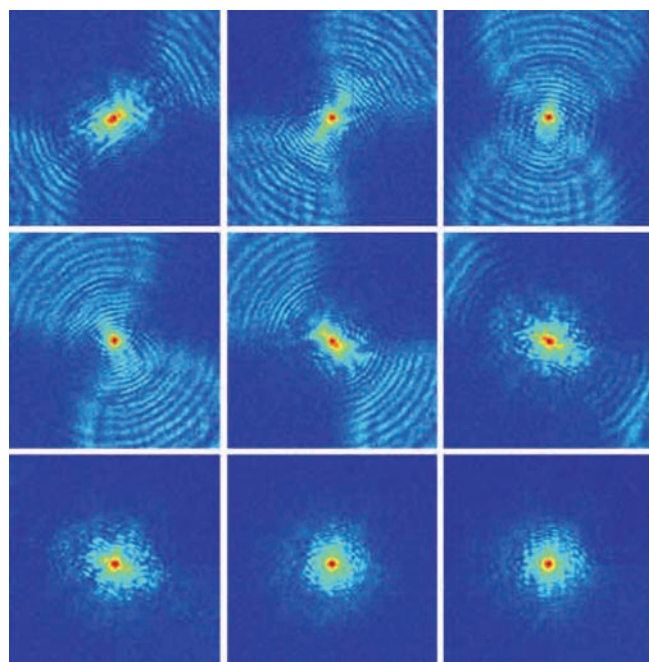
### Ptychography & Coherent Diffractive Imaging

*Ptychographical coherent diffractive imaging* (pCDI) is an extension of the above mentioned iterative phase retrieval methods and relies on collecting a number of Fraunhofer diffraction patterns (Fig. 1 and Fig. 2). Each of these patterns originates from a different but overlapping region of the specimen, which is moved laterally across the illuminating beam (Fig. 3a). The solution strategy is to iteratively reconstruct and refine a single projection image of the sample, which is consistent with all the recorded diffraction patterns. The method is related to a direct, non-iterative solution of the crystallographic phase problem



▲ FIG. 1: Schematic of the experimental setup for lensless ptychographic diffractive imaging. The sample is scanned across the x-ray beam defined by a pinhole aperture and for each sample position a diffraction pattern is recorded by a two-dimensional detector.

► FIG. 2: Nine (out of 225) coherent x-ray diffraction patterns (displayed on logarithmic colorscale) recorded for a micro-structured test sample displayed in Fig. 3a.



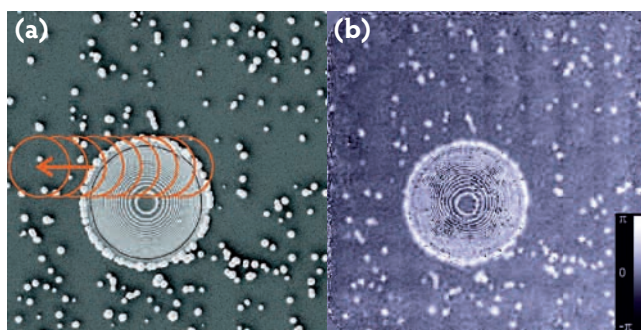
called *ptychography* (from the Greek “πτυξ” meaning “fold” [8]) and was first proposed by Hoppe and Hegerl more than 30 years ago [8,9]. In his pioneering work Hoppe describes how finite coherent illumination can be used to restore the phase information from the interference pattern recorded between the Bragg peaks of a crystalline specimen. The method was further developed for non-periodic objects [10-12], combined with iterative phase retrieval algorithms [13,14] and finally demonstrated with visible light and x-rays [1,2,15]. In the following, we briefly review the basic principles of the method and present some recent results obtained with x-rays and visible laser light.

Prerequisite for pCDI is a well-known, substantially localized and mainly coherent illumination. In the case of x-rays, this can be achieved by placing a small pinhole aperture into a highly brilliant x-ray beam from a third-generation synchrotron source, see Fig. 1. The resulting illumination function, described by the complex-valued probe  $P(r)$ , is then incident on the object, which is characterized by the function  $O(r)$ . For a relative shift,  $r_i$ , between the sample and the illumination function, the resulting exit wave,  $\Psi_i(r) = P(r)O(r-r_i)$ , is propagated onto the Fraunhofer plane (blue arrows in Fig. 4), where the modulus is replaced by the recorded data and the phase is preserved, as is usual in iterative methods. Upon backpropagation (red arrows in Fig. 4), the so-obtained new exit wave  $\Psi_{i,neu}(r)$  differs from the initial exit wave estimate  $\Psi_i(r)$ . The difference between these is used to correct the object function  $O(r-r_i)$  in regions where the probe amplitude has a significant, non-zero value. A cycle over all diffraction patterns corresponds to one iteration step that brings us from the current object estimate,  $O_n(r-r_i)$ , to the input for the next iteration:  $O_{n+1}(r-r_i)$ , where  $n$  labels the number of iteration. The cycle is initiated with a random set of amplitudes and phases in the object function. Convergence of the algorithm is typically obtained after a few tens of iterations and can be monitored by the deviation between measured and calculated intensities via a normalized sum of squared errors.

## Experimental Results

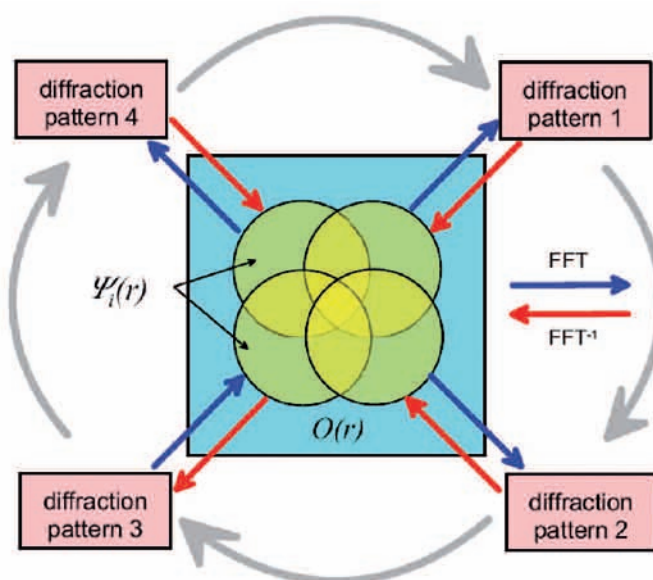
The results shown in Fig. 2 and Fig. 3 were obtained at the Swiss Light Source with monochromatic x-rays with an energy of 6.0 keV ( $\lambda = 0.21$  nm). The beam-defining pinhole aperture of 10  $\mu\text{m}$  diameter (see Fig. 1) was placed at a distance of 35 m from the source. A nano-structured object, a gold Fresnel zone plate, was used as specimen and illuminated at  $15 \times 15$  overlapping positions that were spaced by 3  $\mu\text{m}$ , nine of which are shown in Fig. 3a. The corresponding diffraction patterns (shown in Fig. 2) were recorded with a fibre-coupled CCD detector (Photonic Science Hystar, effective pixel size 4.5  $\mu\text{m}$ ) located 2.25 m downstream from the sample, using an exposure time of 1 sec per position.

The phase of the complex object transmission function that was reconstructed from the 225 diffraction patterns after 20 iterations is shown in Fig. 3b. On the outskirts of the zone plate, *i.e.*, the alternating attenuating and phase shifting concentric rings in the centre of the image, is a random distribution of gold balls ranging from 250 to 1500 nm in diameter. Both the inner ring structure, with periods in the few hundred nanometre range, and the outlying gold balls are clearly visible in the reconstruction.



▲ FIG. 3: Results with X-rays. (a) Scanning electron micrograph of the test sample with gold nanostructures. The circles indicate nine of the 225 pinhole positions for which diffraction patterns were recorded (Fig. 2). (b) Phase of the reconstructed complex-valued exit wave of the specimen (linear colour scale). The images represent a field of view of  $52 \times 52 \mu\text{m}^2$ .

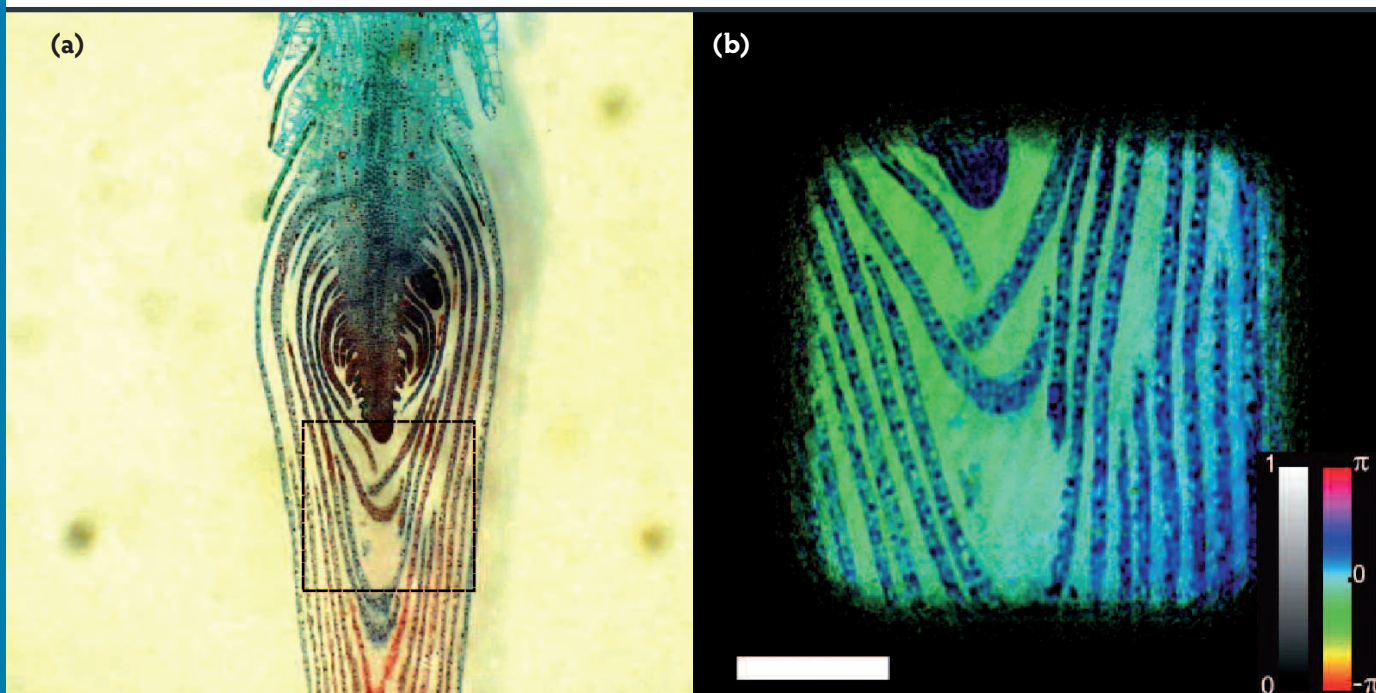
▼ FIG. 4: Schematic of the iterative phase-retrieval algorithm for ptychographical coherent diffractive imaging. The gray circular arrows indicate the iterative loop according to which the diffraction patterns are used to update the object. The blue and red arrows within represent the forward and backward Fourier transforms that link the diffraction patterns with the object.



Importantly, these features are significantly smaller than the diameter of the illumination function ( $\sim 10\ \mu\text{m}$ ) that was used to scan the sample. The image resolution in this reconstruction of about 200 nm was mainly limited by the dynamic range and signal-to-noise ratio of the CCD detector. We believe that in the near future this resolution can be pushed into the several nanometre range by using improved x-ray detectors as, e.g., noiseless, direct-detection x-ray pixel detectors with high dynamic range.

The potential of the method in indeed yielding almost diffraction-limited resolution without using lenses or other optical components was furthermore confirmed by recent experiments with visible laser light [2,15]. Additional results, shown here in Fig. 5, were obtained with a 15 mW HeNe laser, a 200 micron pinhole aperture and a standard cooled 1 Megapixel CCD detector without a single lens in the optical path.  $11 \times 11$  diffraction patterns (with  $50\ \mu\text{m}$  stepsize) were recorded at a distance of 200 mm behind the sample. The reconstructed combined amplitude and phase image of the object is shown in Fig. 5 together with a conventional visible-light micrograph. These results clearly demonstrate both that this method has the potential to yield wavelength limited resolution without relying on the use of an objective and that complex amplitude and phase objects can be reconstructed without significant artefacts or the usual non-uniqueness problems associated with the reconstruction of complex-valued objects. ■

▼ **FIG. 5:** Results with visible laser light. (a) Visible-light micrograph of the stem tip of a hydrilla verticillata. (b) Reconstructed phase and amplitude image from 121 diffraction patterns taken within the area indicated by the dashed square in (a). For the color representation in (b), the amplitude of the reconstructed exit wave of the specimen was assigned to the brightness and the complex phase to the hue in the image. The white scale bar represents 250  $\mu\text{m}$ .



## Acknowledgements:

We gratefully acknowledge J. M. Rodenburg, A. C. Hurst, and A. G. Cullis for many fruitful discussions.

## References

- [1] J.M. Rodenburg, A.C. Hurst, A.G. Cullis, B.R. Dobson, F. Pfeiffer, O. Bunk, C. David, K. Jefimovs, and I. Johnson, *Phys. Rev. Lett.* **98**, 034801 (2007).
- [2] O. Bunk, M. Dierolf, S. Kynde, I. Johnson, O. Marti, and F. Pfeiffer, *Ultramicroscopy*, "doi:10.1016/j.ultramicro.2007.08.003" (2007).
- [3] R.W. Gerchberg and W.O. Saxton, *Optik* **35**, 237 (1972).
- [4] J.R. Fienup, *Appl. Opt.* **21**, 2758 (1982).
- [5] D. Shapiro, P. Thibault, T. Beetz, V. Elser, M. Howells, C. Jacobsen, J. Kirz, E. Lima, H. Miao, A.M. Neiman, and D. Sayre, *Proc. Natl. Acad. Sci. USA* **102**, 15343 (2005).
- [6] M.A. Pfeifer, G.J. Williams, I.A. Vartanyants, R. Harder, and I.K. Robinson, *Nature* **442**, 63 (2006).
- [7] H.N. Chapman, A. Barty, S. Marchesini, A. Noy, S.P. Hau-Riege, C. Cui, M.R. Howells, R. Rosen, H. He, J.C.H. Spence, U. Weierstall, T. Beetz, C. Jacobsen, and D. Shapiro, *J. Opt. Soc. Am. A* **23**, 1179 (2006).
- [8] W. Hoppe, *Acta Cryst. A* **25**, 508 (1969).
- [9] R. Hegerl and W. Hoppe, *Ber. Bunsen-Ges.* **74**, 1148 (1970).
- [10] J.M. Rodenburg and R.H.T. Bates, *Philos. Trans. R. Soc. London A* **339**, 521 (1992).
- [11] P.D. Nellist, B.C. McCallum, and J.M. Rodenburg, *Nature* **374**, 630 (1995).
- [12] H.N. Chapman, *Ultramicroscopy* **66**, 153 (1996).
- [13] H.M.L. Faulkner and J.M. Rodenburg, *Phys. Rev. Lett.* **93**, 023903 (2004).
- [14] J.M. Rodenburg and H.M.L. Faulkner, *Appl. Phys. Lett.* **85**, 4795 (2004).
- [15] J.M. Rodenburg, A.C. Hurst, and A.G. Cullis, *Ultramicroscopy* **107**, 227 (2007).